Supporting Information

Impact of Adsorption on Scanning Electrochemical Microscopy (SECM) Voltammetry and Implications for Nanogap Measurements

Sze-yin Tan,[†‡] *Jie Zhang,*[‡] *Alan M. Bond,*[‡] *Julie V. Macpherson,*[†] *Patrick R. Unwin*[†]*

[†] Department of Chemistry, University of Warwick, Coventry, West Midlands CV4 7AL, United Kingdom

[‡] School of Chemistry, Monash University, Clayton, Victoria 3800, Australia

* To whom correspondence should be addressed. E-mail: p.r.unwin@warwick.ac.uk

Contents

Section S-1: Additional experimental details

SECM Instrumentation

A home-built scanning electrochemical microscope (SECM) was mounted on a vibration-isolation table inside a Faraday cage. The ultramicroelectrode (UME) tip was mounted in a tip holder on a piezo-bender actuator, to which an oscillation (70 Hz with a magnitude of 150 nm (~ 1 % UME tip electrode radius)) was applied. In turn, this was mounted on a 3D-piezoelectric positioner controlled by a PC running custom LabVIEW code (LabVIEW 9.0, National Instruments), which was also used for data acquisition. The tip-substrate separation was controlled by monitoring the damping of the oscillation amplitude of the UME tip upon intermittent contact between the tip and surface (typically 5 %).

Adsorption of $FcTMA^+$ and $FcTMA^{2+}$ to Glass

Bulk electrolysis of $FcTMA^+$ solutions (1 M KCl) was carried out quantitatively (monitored by steady-state voltammetry at a 12.5 μm-radius Pt UME tip) in a two compartment cell. Both compartments were filled with known concentrations of $FcTMA^+$ solution separated by a P4 frit to minimize mixing of the solutions in the separate compartments. Two carbon fiber felt cloths of large area served as the working and counter electrodes in the separate compartments. An AgCl-coated Ag wire reference electrode was placed into the same compartment as the working electrode and a working electrode bias of 0.8 V was applied to electrochemically-generate $FcTMA^{2+}$.

To probe the possible adsorption of $FcTMA^+$ and $FcTMA^{2+}$ to glass, UME voltammetry in a drop of solution on a glass surface was employed, which provides a reasonably high surface area-to-volume ratio to be able to detect relatively low surface coverages.[1] A UME was manually lowered close to a glass substrate surrounded by a moat of water to minimize droplet evaporation. A 3.5 μL drop of $FcTMA^+$ or $FcTMA^{2+}$ solution (1 M

KCl) of known concentration was placed onto the glass substrate positioned below the UME. The typical area of glass covered by the drop was 0.14 cm^2. Following the deposition of the droplet, sufficient time must be allowed for the adsorption process to attain equilibrium and, particularly, for the diffusion front to propagate through the droplet so that the concentration of solute in the droplet becomes uniform.[1] The diffusion-limited current measured at the UME, which was typically 0.5 mm from the glass surface, was used to monitor the concentration of $FcTMA^+$ or $FcTMA^{2+}$ (solute) in the droplet (in separate experiments). Knowing the initial and final concentration values allowed an estimation of solute adsorbed on the surface compared to that remaining in bulk solution.[1]

Section S-2: Cyclic voltammetry at highly oriented pyrolytic graphite

Figure S-1 (a) shows a plot of ΔE_p versus scan rate, v. ΔE_p decreases with increasing v as the mixed diffusion-adsorption process becomes increasingly biased towards the adsorbed species. Analysis of CVs for the oxidation of $FcTMA^+$ on HOPG further revealed larger forward wave peak currents compared to the reverse peak currents (Figure S-1 (b)) with the difference increasing with increasing v. This is indicative of the weak adsorption of $FcTMA^+$ onto the HOPG electrode. Figure S-1 (c) shows a comparison of an experimental voltammogram to a simulated diffusion-controlled response at a v = 10 V s^{-1}. The planar diffusion simulations were carried out with the MECSim (Monash Electrochemistry Simulator) computer program written in Fortran[2] (see caption for simulation parameters) using fitting procedures described in reference 3.[3] The much higher current on the forward scan, seen experimentally, is indicative of the oxidation of electrode-adsorbed $FcTMA^+$, as well as $FcTMA^+$ from solution.

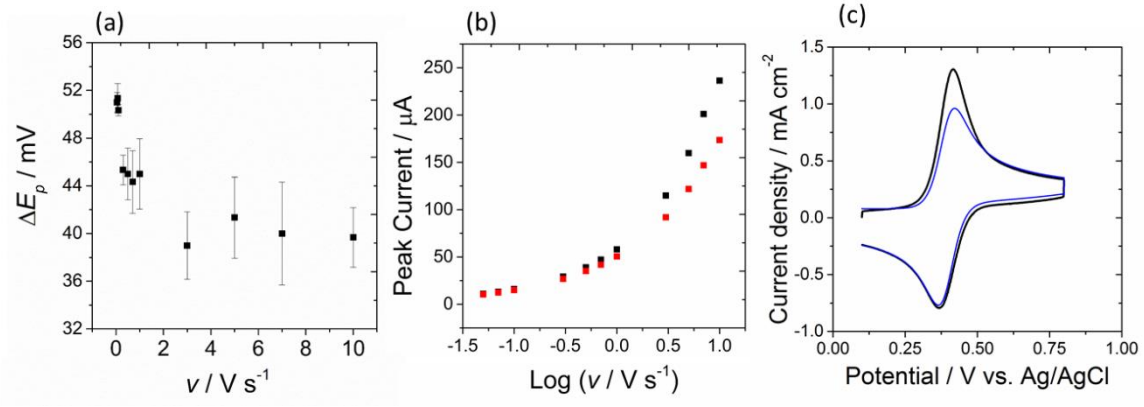

Figure S-1. (a) Plot of ΔE_p vs. v. (b) Plot of forward peak currents (black) and reverse peak currents (red) vs. log v. (c) Experimental voltammogram (black) compared to the corresponding simulated diffusional wave (blue) at v = 10 V s^{-1}. Simulation parameters: k^0 = 100 cm s^{-1} (reversible), α = 0.5, A = 0.165 cm^2 (area of droplet calculated using procedure in reference 3)[4], D_{FcTMA^+} = 6.7 × 10^{-6} cm^2 s^{-1} and $D_{FcTMA^{2+}}$ = 6.1 × 10^{-6} cm^2 s^{-1}, C_{dl} = 8 µF cm^{-2}.

Section S-3: Simulated SECM voltammograms for a 12.5 µm-radius UME tip

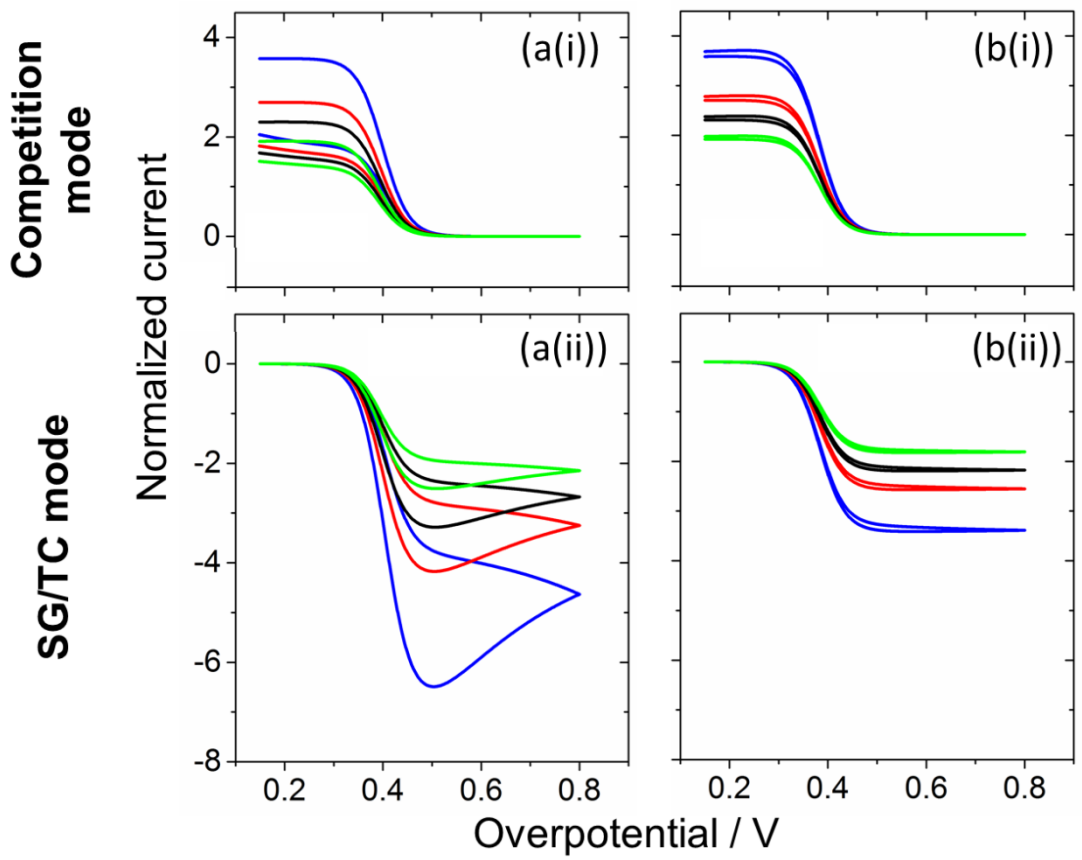

Figure S-2. Simulated substrate voltammetry SECM tip current-substrate potential responses for the competition (i) and SG/TC (ii) modes for a one-electron oxidation process at the substrate electrode at different normalized tip-substrate distances (L = 0.209 (blue), 0.297 (red), 0.367 (black) and 0.478 (green)) for (a) adsorption of reactant (present in bulk at a concentration of 0.4 mM) occurs on the substrate electrode (reverse potential sweeps produce lower currents compared to the forward potential sweep) and (b) a typical adsorption-free case is considered. Simulation parameters: k^0_{UME} = 25 cm s^{-1} (reversible), k^0_{HOPG} = 10 cm s^{-1} (reversible), $E^{0`}$ = 0.38 V, D_{FcTMA^+} = 6.7 × 10^{-6} cm^2 s^{-1}, $D_{FcTMA^{2+}}$ = 6.1 × 10^{-6} cm^2 s^{-1}, Γ_{HOPG} = 1.13 × 10^{-10} mol cm^{-2} and $K_{ads,HOPG}$ = 7.4 × 10^5 cm^3 mol^{-1}.

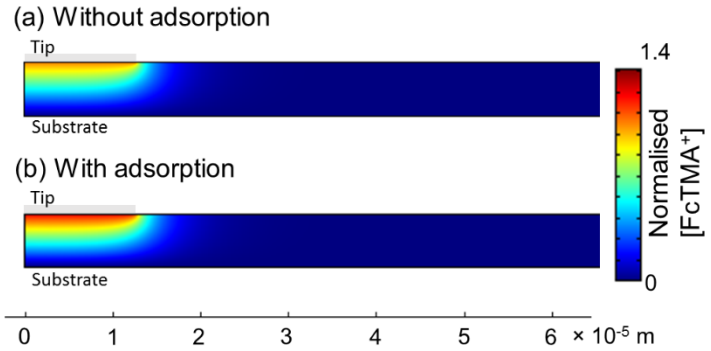

Figure S-3. Concentration profiles of $FcTMA^+$ under the tip at E_{HOPG} = 0.5 V on the forward sweep for the SG/TC mode (a) without and (b) with $FcTMA^+$ adsorption on the SECM substrate.

Section S-4: Determination of the diffusion coefficient of $FcTMA^+$

CVs for the oxidation of 1.5 mM $FcTMA^+$ (1 M KCl) (Figure S-4) gave voltammograms which were close to reversible on the time-scale of steady-state UME voltammetry. The measured diffusion-limited current (forward wave) gave a diffusion coefficient, D_{FcTMA^+} = $(6.74 \pm 0.03) \times 10^{-6}$ cm^2 s^{-1} with $E_{1/2}$ of 0.38 ± 0.01 V vs. Ag/AgCl (1 M KCl).

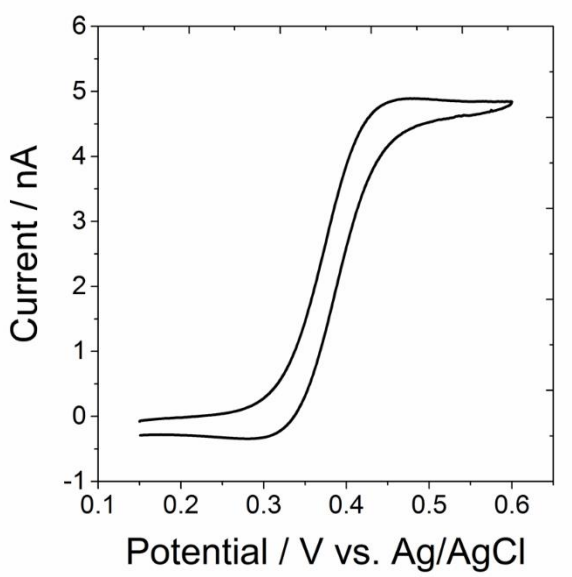

Figure S-4. Typical CV for the oxidation of 1.5 mM $FcTMA^+$ in 1 M KCl supporting electrolyte at a 12.5 µm-radius Pt UME at a scan rate of 50mV s^{-1}.

Section S-5: Determination of the diffusion coefficient of $FcTMA^{2+}$

Although voltammetric studies usually assume the same *D* value for both oxidized and reduced forms of a redox couple,[5] this is rarely the case and accurate determination of these values can be very important for quantitative kinetic studies,[6–9] especially if one is looking at measuring the kinetics of fast processes that are close to the diffusion-limit.

In order to accurately determine *D* of $FcTMA^{2+}$, we employed SECM-chronoamperometric measurements with a 12.5 μm-radius Pt UME in both the feedback[6] and SG/TC[7] mode. The responses can be analyzed to give the ratio of diffusion coefficients of the oxidized to reduced form of a redox mediator couple, γ, when the redox couple undergoes a simple diffusion-controlled one-electron transfer, without any kinetic complications and adsorption effects.[6,7]

Under feedback conditions, γ has no effect on the steady-state current but can affect the way steady-state in reached.[7] Therefore, the normalized steady-state limiting-current determined in the feedback mode can be used to determine precisely the tip-substrate separation for the pair of feedback and SG/TC steady-state limiting tip currents taken at the same height. Under SG/TC conditions, $FcTMA^{2+}$ is electrogenerated at a diffusion-controlled rate from the precursor in bulk solution, $FcTMA^{+}$, at a Pt macroscopic substrate:

Substrate reaction: $FcTMA^{+} \xrightarrow{-e^-} FcTMA^{2+}$ (S-1)

$FcTMA^{2+}$ diffuses away from the substrate and part of the diffusion field is intercepted by the UME tip. At the UME, $FcTMA^{2+}$ undergoes a diffusion-controlled reduction to $FcTMA^{+}$:

Tip reaction: $FcTMA^{2+} \xrightarrow{+e^-} FcTMA^{+}$ (S-2)

Although the macroscopic substrate electrode will have a transient form, the redox mediator diffusional cycling between the tip and substrate attains a quasi-steady-state. A simple modification of an empirically derived equation for the positive feedback mode[10] can be used to describe the normalized steady-state collection current-distance data:

$$I = \gamma\left[0.68 + 0.78377/L + 0.3315\exp(-1.0672L)\right] \qquad \text{(S-3)}$$

where I is the normalized current measured at the UME tip, γ is the diffusion coefficient ratio of oxidized to reduced forms of the redox couple and L is the normalized distance between the tip and substrate. γ was found to be 0.91 from best fit.

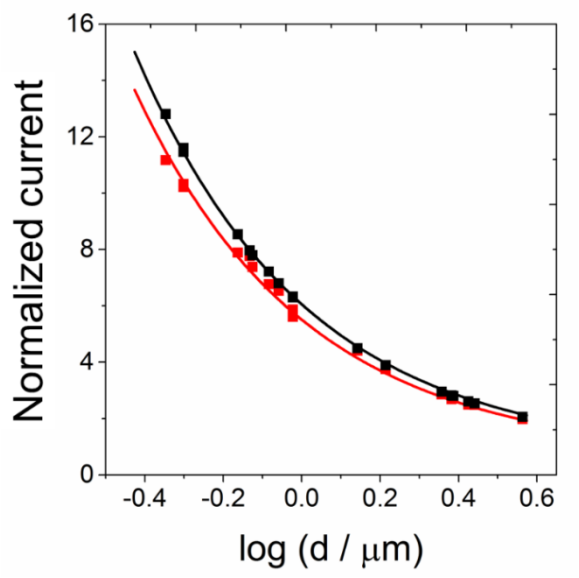

Figure S-5. Steady-state feedback (black) and SG/TC (red) normalized UME tip current vs. distance characteristics for the $FcTMA^{+/2+}$ redox couple. The dotted line represents experimental results and solid lines indicate the γ-independent steady-state theory (black) and the theoretical SG/TC behavior for γ = 0.91 (red).

Section S-6: Cyclic voltammetry at ‘aged’ highly oriented pyrolytic graphite electrodes

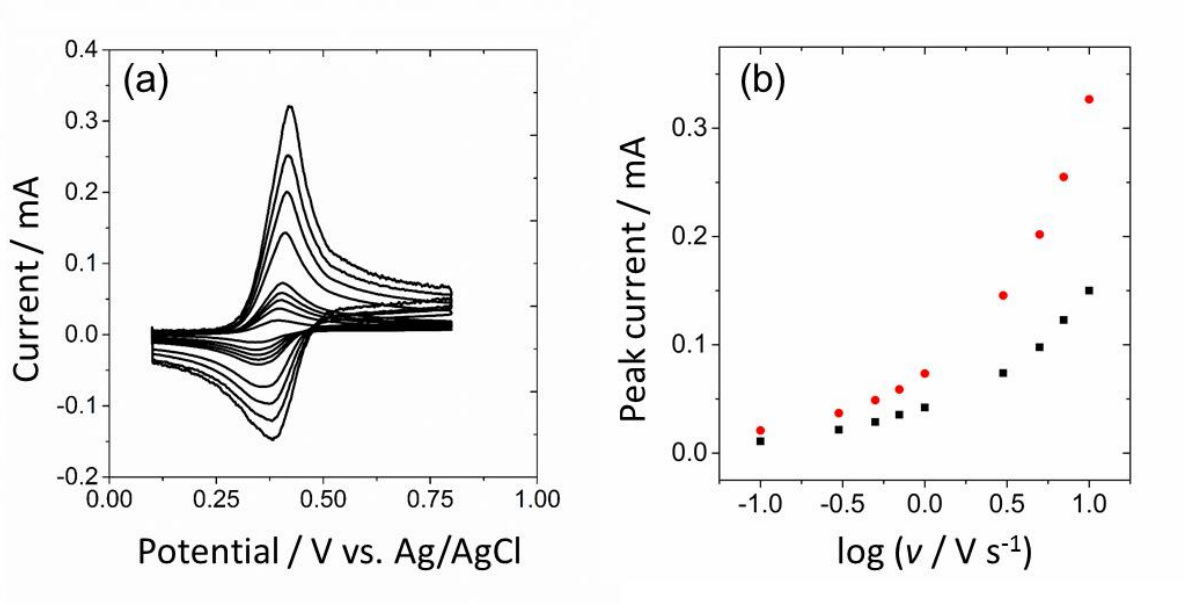

Figure S-6. (a) CVs for the oxidation of 0.4 mM $FcTMA^+$ (1 M KCl) at ‘aged’ (1 hour exposure to air) ZYA grade HOPG in the droplet configuration (area of droplet was 0.162 cm^2). $E_{1/2,app}$ was found to be 0.38 V vs. Ag/AgCl (1 M KCl) with ΔE_p = 48 ± 6 mV (for all scan rates employed). (b) A plot of forward (red) and reverse (black) peak currents at different scan rate values. The peak current difference increases with increasing scan rate and is larger than at freshly cleaved HOPG surfaces (see Figure S-1 (b)). The surface coverage was estimated to be *ca*. 2.0 × 10^{-10} mol cm^{-2} with 0.4 mM $FcTMA^+$ in bulk solution.

Section S-7: Determination of $FcTMA^+$ and $FcTMA^{2+}$ adsorption on glass

An UME was used to monitor amperometrically the concentration of either $FcTMA^+$ or $FcTMA^{2+}$ (in separate experiments) in a small droplet of solution (3.5 µL) placed on a glass surface where the concentrations can be determined from measurements of the diffusion-limited current, i_{UME}. The droplet of solution was surrounding by a moat of supporting electrolyte solution to prevent evaporation.[1]

A decrease in limiting current, Δi_{UME} can be ascribed to analyte adsorption onto the glass surface, Γ_{glass} (mol cm^{-2}):[1]

$$\Gamma_{glass} = (V / A)(\Delta i_{UME} / 4nFa_{UME}D_i) \qquad \text{(S-4)}$$

where V is the volume of the drop and A is the glass area of which it covers.

As shown in Figure S-7 (a), there was essentially no change in i_{UME} measured in a drop of $FcTMA^+$ solution on glass. In contrast, $FcTMA^{2+}$ evidently adsorbed much more strongly on glass surfaces. The $FcTMA^{2+}$ adsorption data fitted reasonably well to a Langmuir isotherm (over the concentration range of the experiment), Figure S-7 (b), with $\Gamma^0_{glass} = 2.3 \pm 0.8 \times 10^{-9}$ mol cm^{-2} and $K_{ads,glass} = 2.6 \pm 0.4 \times 10^6$ cm^3 mol^{-1}.

The strong adsorption on glass of $FcTMA^{2+}$ compared to $FcTMA^+$ may seem surprising, but other divalent cation molecules, such as tris (2,2'-bipyridine) ruthenium (II) strongly adsorbs from aqueous on glass at similar neutral pH to these measurements, especially at higher electrolyte concentration.[11] The much stronger adsorption of multivalent cations compared to monovalent ions, and the enhancement by supporting electrolyte is well-established.[12,13]

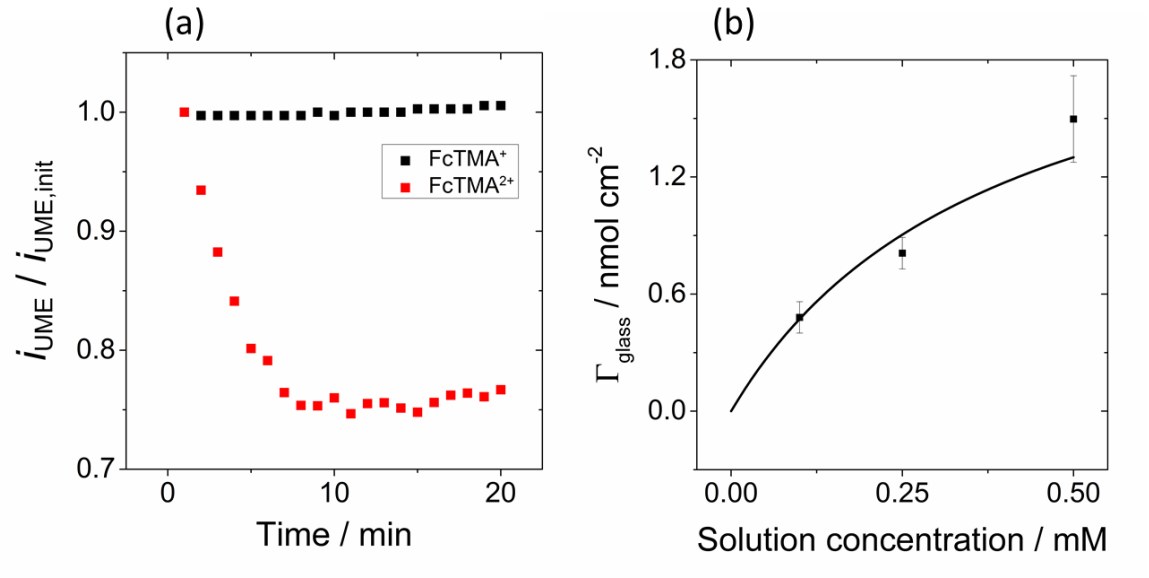

Figure S-7. (a) Data showing the change in concentration in a 3.5 µL droplet of $FcTMA^{+}$ (black) and $FcTMA^{2+}$ (red) solution on glass. (b) Amount of $FcTMA^{2+}$ adsorbed on glass, Γ_{glass} as a function of remaining solution concentration of $FcTMA^{2+}$.

Section S-8: Additional simulation details

As shown experimentally, $FcTMA^{2+}$ adsorbs onto glass surfaces, which can be represented by the following:

$$FcTMA^{2+}_{soln} \underset{k_{des,glass}}{\overset{k_{ads,glass}}{\rightleftharpoons}} FcTMA^{2+}_{ads} \qquad \text{(S-5)}$$

where $k_{ads,glass}$ and $k_{des,glass}$ are the rate constants for the adsorption and desorption of $FcTMA^{2+}$ onto the glass sheath surrounding the Pt UME tip.

In the SECM experiments, for $t > 0$, the flux due to adsorption of the $FcTMA^{2+}$ at the glass sheath ($a_{UME} < r < a_{UME} \times RG$, $z = d$) is defined by:

$$-\mathbf{n}.\mathbf{N}_{FcTMA^{2+},glass} = -\Gamma^{0}_{glass}\left[k_{ads,glass}(1-\theta_{glass})c_{FcTMA^{2+}_{soln}} - k_{des,glass}\theta_{glass}\right] \qquad \text{(S-6)}$$

where Γ^{0}_{glass} is the saturation value at maximum surface concentration, determined to be 2.3×10^{-9} mol cm^{-2} (from glass adsorption experiments, see Section S-7), the equilibrium adsorption constant for the glass surface, $K_{ads,glass} = \frac{k_{ads,glass}}{k_{des,glass}}$ was found to be 2.6×10^{6} mol cm^{-3} from experiments described herein (reasonably assuming a Langmiurian isotherm) with $k_{ads,glass}$ set sufficiently large as to maintain equilibrium (1×10^{9} cm^{3} mol^{-1} s^{-1}), which is reasonable for this process which involves mainly Van der Waals electrostatic interactions of $FcTMA^{2+}$ with the surface. θ_{glass} is the fractional surface coverage of $FcTMA^{2+}$ on the glass.

Redox mediators immobilized onto the glass (non-conducting) surface can undergo various charge transfer processes, such as direct electron transfer (ET) between surface and redox molecules in the solution and charge exchange between the redox active species which are immobilized along the surface.[14–18] In order to account for this in a simple manner, we

introduced a species, $FcTMA^{2+*}$ generated in solution by reaction at the glass surface through the following ET process:

$$FcTMA^{+}_{soln} \xrightarrow{K_{12}} FcTMA^{2+*}_{soln} \quad \text{(S-7)}$$

where K_{12} is the $FcTMA^{+/2+}$ homogeneous self-exchange rate constant (9×10^6 M^{-1} s^{-1}).[19]

For $t > 0$, the flux due to the redox reaction of $FcTMA^{+}$ in solution producing $FcTMA^{2+*}$ via reaction at the glass sheath is defined by:

$$-\mathbf{n}.\mathbf{N}_{FcTMA^{+},glass} = -K_{12} c_{FcTMA^{+}_{soln}} \Gamma^{0}_{glass} \theta_{glass} \quad \text{(S-8)}$$

$$-\mathbf{n}.\mathbf{N}_{FcTMA^{2+*},glass} = -\left[-K_{12} c_{FcTMA^{+}_{soln}} \Gamma^{0}_{glass} \theta_{glass} \right] \quad \text{(S-9)}$$

Here, the $FcTMA^{+}$ species in solution can be oxidized by surface-confined $FcTMA^{2+}$ species on the glass (the glass surface assumed to be unchanged by the ET process) to generate the $FcTMA^{2+*}$ species. This is labeled as such, as it does not participate in any glass adsorption processes, and diffuses away from the glass surface for detection at the tip electrode (in substrate voltammetry experiments). This simplification is reasonable for the demonstrative proposes herein given the well-known fast lateral charge propagation within surface attached molecules,[12-18] especially ferrocenes at high surface coverage,[13] which would rapidly restore $FcTMA^{+}$ produced in the charge transfer reaction back to $FcTMA^{2+}_{ads}$. Furthermore, the sharp concentration gradient in the solution near the tip/glass boundary makes it reasonable to assume that any flux of $FcTMA^{2+}$ species generated from this process at the glass surface will quickly diffuse away and will then contribute to the flux at the substrate or tip electrode.

Section S-9: Kinetic analysis of nanogap SECM simulations

Table S-1. Fitting parameters from Figure 5 (a) in the main text, L = 0.1 and $\Delta E^{0`} = E^{0`}_{app} - E^{0`}$.

Simulated data	**Adsorption-free fitting**					
$\Gamma_{HOPG,FcTMA^+}$ / **mol cm^{-2}**	$\Delta E^{0`}$ / **mV**		k^0_{app} / **cm s^{-1}**		d_{app} / **nm**	
	Competition mode	**SG/TC mode**	**Competition mode**	**SG/TC mode**	**Competition mode**	**SG/TC mode**
0	0	0	5	5	50	50
1.1 ×10^{-10} (22 %)	4	0	5	≥14	50	49
1.53×10^{-10} (30 %)	4	0	4.8	≥14	50	48
2.0 ×10^{-10} (40 %	4	0	4.6	≥14	50	47
2.6 ×10^{-10} (50 %)	4	0	4.0	≥14	50	46

Table S-2. Fitting parameters from Figure 7 (a) in the main text, L = 0.1.

Simulated data	**Adsorption-free fitting**					
k^0 / **cm s^{-1}**	$\Delta E^{0`}$ / **mV**		k^0_{app} / **cm s^{-1}**		d_{app} / **nm**	
	Competition mode	**SG/TC mode**	**Competition mode**	**SG/TC mode**	**Competition mode**	**SG/TC mode**
10	3	0	5	≥14	53	45
5	3	-5	3	≥14	53	45
1	0	-6	0.8	1.2	53	46
0.5	-9	-9	0.5	0.5	53	47

Table S-3. Fitting parameters from Figure 7 (b) in the main text, k^0 = 5 cm s^{-1}

Simulated data	**Adsorption-free fitting**					
L	$\Delta E^{0`}$ / **mV**		k^0_{app} / **cm s^{-1}**		d_{app} / **nm**	
	Competition mode	**SG/TC mode**	**Competition mode**	**SG/TC mode**	**Competition mode**	**SG/TC mode**
0.1	3	-5	3.0	≥15	53	45
0.15	3	-7	3.0	≥10	83	66
0.2	3	-10	2.2	≥8	117	83
0.25	2	-12	1.9	≥7	154	99
0.3	2	-15	1.6	≥6	190	112

References

(1) Unwin, P.; Bard, A. *Anal. Chem.* **1992**, *64*, 113–119.

(2) Bond, A. M.; Duffy, N. W.; Elton, D. M.; Fleming, B. D. *Anal. Chem.* **2009**, *81*, 8801–8808.

(3) Sher, A. A.; Bond, A. M.; Gavaghan, D. J.; Harriman, K.; Feldberg, S. W.; Duffy, N. W.; Guo, S.-X.; Zhang, J. *Anal. Chem.* **2004**, *76* (21), 13.

(4) Cuharuc, A. S.; Zhang, G.; Unwin, P. R. *Phys. Chem. Chem. Phys.* **2016**, (Just Accepted).

(5) Nioradze, N.; Chen, R.; Kurapati, N.; Khvataeva-Domanov, A.; Mabic, S.; Amemiya, S. *Anal. Chem.* **2015**, *87*, 4836–4843.

(6) Martin, R. D.; Unwin, P. R. *J. Electroanal. Chem.* **1997**, *439*, 123–136.

(7) Martin, R. D.; Unwin, P. R. *Anal. Chem.* **1998**, *70*, 276–284.

(8) Nioradze, N.; Kim, J.; Amemiya, S. *Anal. Chem.* **2011**, *83*, 828–835.

(9) Mampallil, D.; Mathwig, K.; Kang, S.; Lemay, S. G. *Anal. Chem.* **2013**, *85*, 6053–6058.

(10) Mirkin, M. V.; Fan, F.-R. F.; Bard, A. J. *J. Electroanal. Chem.* **1992**, *328*, 47–62.

(11) Powell, H. V; Schnippering, M.; Mazurenka, M.; Macpherson, J. V; Mackenzie, S. R.; Unwin, P. R. *Langmuir* **2009**, *25*, 248–255.

(12) Tadros, T. F.; Lyklema, J. *J. Electroanal. Chem. Interfacial Electrochem.* **1968**, *17*, 267–275.

(13) Porus, M.; Labbez, C.; Maroni, P.; Borkovec, M. *J. Chem. Phys.* **2011**, *135*, 064701.

(14) Zhang, J.; Slevin, C. J.; Morton, C.; Scott, P.; Walton, D. J.; Unwin, P. R. *J. Phys. Chem. B.* **2001**, *105*, 11120–11130.

(15) Zhang, J.; Unwin, P. R. *J. Am. Chem. Soc.* **2002**, *124*, 2379–2383.

(16) Mullane, A. P. O.; Macpherson, J. V; Unwin, P. R.; Cervera-Montesinos, J.; Menzanares, J. A.; Frehill, F.; Vos, J. G. *J. Phys. Chem. B.* **2004**, *108*, 7219–7227.

(17) Whitworth, A. L.; Mandler, D.; Unwin, P. R. *Phys. Chem. Chem. Phys.* **2005**, *7*, 356–365.

(18) Hauquier, F.; Ghilane, J.; Fabre, B.; Hapiot, P. *J. Am. Chem. Soc.* **2008**, *130*, 2748–2749.